JGR Biogeosciences

RESEARCH ARTICLE
10.1029/2019JG005394

Key Points:
- Terrestrial signal has been found in coral skeletal Ba/Ca, $\delta^{18}O$, and to a less extent in $\delta^{13}C$
- Delayed responses of seawater and coral chemistry to river discharge are likely results of tide-dominated hydrodynamics
- Enhanced freshwater and sediments transports to the nearshore Kimberley since 1920s linked to the strengthening of monsoon precipitation

Supporting Information:
- Supporting Information S1

Correspondence to:
X. Chen,
chenxf@gig.ac.cn

Citation:
Chen, X., Deng, W., Wei, G., & McCulloch, M. (2020). Terrestrial signature in coral Ba/Ca, $\delta^{18}O$, and $\delta^{13}C$ records from a macrotide-dominated nearshore reef environment, Kimberley region of northwestern Australia. *Journal of Geophysical Research: Biogeosciences*, *125*, e2019JG005394. https://doi.org/10.1029/2019JG005394

Received 24 JUL 2019
Accepted 19 NOV 2019
Accepted article online 12 JAN 2020

Terrestrial Signature in Coral Ba/Ca, $\delta^{18}O$, and $\delta^{13}C$ Records From a Macrotide-Dominated Nearshore Reef Environment, Kimberley Region of Northwestern Australia

Xuefei Chen[1,2], Wenfeng Deng[1,2], Gangjian Wei[1,2], and Malcolm McCulloch[3,4]

[1]State Key Laboratory of Isotope Geochemistry, Guangzhou Institute of Geochemistry, Chinese Academy of Sciences, Guangzhou, China, [2]Southern Marine Science and Engineering Guangdong Laboratory, Guangzhou, China, [3]Oceans Graduate School and Oceans Institute, The University of Western Australia, Crawley, Australia, [4]ARC Centre of Excellence for Coral Reef Studies, The University of Western Australia, Crawley, Australia

Abstract The geochemistry preserved in massive scleractinian corals has long been used as proxies for river runoff, but its reliability in naturally extreme environment (i.e., strong hydrodynamics and intensive thermal stress) has not been tested yet. Using *Porites* coral collected from the macrotidal nearshore Kimberley region of northwestern Australia, we assess the impacts of river runoff and associated changes in this extreme environment using elemental (Ba/Ca) and isotopic ($\delta^{18}O$ and $\delta^{13}C$) compositions at both near monthly and annual resolutions. On the monthly timescales, significant terrestrial signatures were noted in skeletal Ba/Ca, $\Delta\delta^{18}O$, and to a lesser extent in $\delta^{13}C$ time series, highlighting their linkage to runoff input of Fitzroy River. However, all the geochemical time series as well as the observational coastal sea surface salinity exhibited a consistent ~1- to 2-month lag with river discharge, possibly a manifestation of the sluggish water and sediments exchange in King Sound which are likely induced by strong tidal forcing. On the annual timescales, Ba/Ca follows the variation in river discharge, while freshwater supplied by both runoff and rainfall all contributed to $\delta^{18}O$ variations. In contrast, annual $\delta^{13}C$ is mainly dominated by the ^{13}C Suess effect, showing a gradually downward trend. Importantly, we find that $\delta^{18}O$ and Ba/Ca records exhibit consistent and significant long-term trends, with $\delta^{18}O$ being decreasing and Ba/Ca being increasing, coupled with the increased Australian monsoon, indicating that strengthened monsoon precipitation has likely brought more freshwater and sediment loads to the nearshore Kimberley region.

Plain Language Summary The geochemistry preserved in massive corals living in the coastal and nearshore region can provide reliable records for terrestrial input of freshwater and sediment. This capacity is not compromised even in highly dynamic, naturally extreme reef environment as revealed in this study. Using elemental (Ba/Ca) and isotopic ($\delta^{18}O$ and $\delta^{13}C$) compositions of a long-lived *Porites* coral from the nearshore Kimberley region of northwestern Australia, we evaluated the runoff-related signals in both monthly and annual coral geochemical records, to explore their possibility being freshwater and sediments tracers. The seasonal Ba/Ca peaks are found to follow the large discharge events, and monthly $\Delta\delta^{18}O$ variation is associated with the changes of coastal salinity driving by the influx of freshwater supplied by Fitzroy River. Terrestrial signal is less manifested in skeletal $\delta^{13}C$ records. Additionally, a consistent ~1- to 2-month temporal lag was found in monthly records, a manifestation of sluggish exchange of water and sediment in this embayment which is likely induced by tidal forcing. The long-term increase in Ba/Ca baseline ratios and decrease in $\delta^{18}O$ from the 1920s onwar, pointed to an enhanced freshwater and sediment loads into the embayment, possibly linking to the lasting strengthening of Australian monsoon. These findings highlight that corals living in the naturally extreme environment can provide reliable records for freshwater and terrestrial sediments transport to the nearshore region by using skeletal $\delta^{18}O$ and Ba/Ca.

1. Introduction

Elemental and isotopic records preserved in scleractinian corals growing in coastal and estuarial regions can provide historical records of the variability of river runoff and terrestrial inputs into the nearshore environments over weekly to centennial timescales, enabling us to evaluate long-term impacts of terrestrial runoff of sediments, nutrients, and pollutants on both coastal waters and coral reefs, especially in the context of

anthropogenic activities and climate changes (e.g., Deng et al., 2013; Grove et al., 2012; Horta-Puga & Carriquiry, 2012; Lewis et al., 2007, 2012, 2018; Lough et al., 2015; McCulloch et al., 2003; Moyer et al., 2012; Nguyen et al., 2013; Prouty et al., 2008, 2010; Saha et al., 2016; Saha, Rodriguez-Ramirez, et al., 2018; Sinclair & McCulloch, 2004). Additionally, this information also serves as valuable evidence of the exchange of waters, solutes, and sediments in the estuaries and coastal oceans, and how these exchanges are affected by winds, tides, and river runoff, especially for regions where continuous monitoring is lacking (Grove et al., 2012; Maina et al., 2012).

Skeletal Ba/Ca ratios are the most commonly used proxy to constrain historical changes in terrestrial inputs (e.g., Alibert et al., 2003; Fallon et al., 1999; Grove et al., 2013; Jupiter et al., 2008; Lewis et al., 2007, 2018; McCulloch et al., 2003; Prouty et al., 2010; Saha et al., 2016, Saha, Rodriguez-Ramirez, et al., 2018; Sinclair & McCulloch, 2004; Walter et al., 2013), despite that uncertainty associated with this proxy remains enigmatic in that seasonal cycles or anomalous peaks of coral Ba/Ca were occasionally reported to decouple from terrestrial runoff (Chen et al., 2011; Lewis et al., 2012, 2018; Saha, Webb, et al., 2018; Tanzil et al., 2019; Sinclair, 2005; Tudhope et al., 1996). In the open ocean, barium is a nutrient-like element with its abundance depleted in the surface ocean but enriched in the deep waters (Chow & Goldberg, 1960; Wolgemuth & Broecker, 1970). However, in the most coastal waters, river runoff is the major source for Ba (Coffey et al., 1997), transporting high concentrations of dissolved Ba and sediment-adsorbed Ba into the nearshore environment. The sediment-adsorbed Ba would desorb from the carrier when encountering high salinity water, as a result of higher ionic strength of seawater, thus increasing the Ba concentrations in the ambient waters subject to sediment influxes such as estuaries and coastal regions (Carroll et al., 1993; Edmond et al., 1978; Moore & Shaw, 2008; Walther & Nims, 2015). Such changes can be well preserved by corals growing in the coastal region, since Ba is thought to be incorporated into the lattice of coral calcareous skeleton with the Ba/Ca ratio being incorporated in proportion to its abundance in seawater (Gonneea et al., 2017; LaVigne et al., 2016). Therefore, it is commonly found that high-resolution Ba/Ca ratios in massive coral skeletons (e.g., *Porites* spp.) exhibit variability that corresponds to enhanced sediment from terrestrial runoff periods which are often particularly prominent during heavy rainfall events (e.g., Alibert et al., 2003; McCulloch et al., 2003; Shen & Sanford, 1990). Furthermore, its baseline concentration shifts can also serve as robust evidence of the long-term effects of human activities on coastal waters, such as land use, pastoral industry, and coastal development (e.g., Lewis et al., 2007; McCulloch et al., 2003; Nguyen et al., 2013; Prouty et al., 2008).

In addition to Ba/Ca ratios, skeletal isotopic "fingerprints" such as $\delta^{18}O$ and $\delta^{13}C$ can also aid in tracking riverine plumes in coastal environments (e.g., Deng et al., 2013; Grove et al., 2012; Moyer et al., 2012). Basically, $\delta^{18}O$ and $\delta^{13}C$ of dissolved inorganic carbon ($\delta^{13}C_{DIC}$) in river water are much isotopic depleted compared to those in seawater (Fairbanks, 1982; Sackett et al., 1997). As a result, seawater $\delta^{18}O$ and $\delta^{13}C_{DIC}$ would decrease during the heavy runoff period. These isotopic signatures can then be partially inherited by the coral as seawater provides the primary material for $CaCO_3$ precipitation, enabling skeletal $\delta^{18}O$ and $\delta^{13}C$ being tracers for freshwater fluxes (or salinity changes) and terrestrial DIC input, respectively (e.g., Cole et al., 1993; Deng et al., 2009, 2013; Felis et al., 2009; Gagan et al., 1998; Guo et al., 2016; Hendy et al., 2002; McCulloch et al., 1994; Moyer et al., 2012; Swart et al., 1999).

However, cautions are still required in interpretation of these coral-based proxies, for that multiple factors are playing competing roles in their fractionation in coral skeletons. For coral $\delta^{18}O$, it is controlled by both temperature and seawater $\delta^{18}O$ ($\delta^{18}O_{sw}$). Therefore, temperature influence should be first constrained before taking $\delta^{18}O_{coral}$ as a freshwater or salinity proxy. This is commonly achieved by subtracting the temperature contribution from the $\delta^{18}O_{coral}$ utilizing either satellite record or coral Sr/Ca temperature proxy (Gagan et al., 1998; McCulloch et al., 1994). As for coral Ba/Ca, the scenario is more complicated due to the complexity of biogeochemistry of Ba in coastal coral skeletons (Chen et al., 2011; Lewis et al., 2018; Saha, Webb, et al., 2018; Sinclair, 2005; Tanzil et al., 2019). Monthly variability of coral Ba/Ca is not only always corresponded to river discharge peaks during wet season but would also show seasonal cycles or anomalously episodic spikes possibly linked to upwelling (Alibert & Kinsley, 2008; Lea et al., 1989), submarine groundwater (Alibert et al., 2003; Jiang et al., 2018), biological activity (Gillikin et al., 2006; Lewis et al., 2018; Saha, Webb, et al., 2018; Sinclair, 2005; Wyndham et al., 2004), anomalously lower temperature (Chen et al., 2011), or sediment resuspension (Alibert et al., 2003; Esslemont et al., 2004). Similarly, coral $\delta^{13}C$ also has limitations as an environmental proxy as drivers such as internal carbon source, coral-symbionts metabolism, kinetic effects, and

other environmental variables may vary case by case (e.g., Allison & Finch, 2012; Deng et al., 2013; Grottoli, 2002; McConnaughey et al., 1997; McConnaughey, 2003; Swart, Healy, et al., 1996; Swart, Leder, et al., 1996). For this reason, skeletal $\delta^{13}C$ can follow the variability with temperature, light availability, or river discharge, but could also show little connection with either of them. As a whole, the geographic and oceanographic conditions, even the coral itself, are critical to the reliability of these coral-based proxies for terrestrial input.

In this study, we examine the utility of coral Ba/Ca, $\delta^{18}O$, and $\delta^{13}C$ as terrestrial/river runoff tracers in a strongly tide-dominated estuary, King Sound of Kimberley region in the northwestern Australia. This region is characterized by some of the largest tidal cycles (up to 12 m) as well as thermally extreme environments modulated by the tidal regime (Dandan et al., 2015; Richards et al., 2015; Schoepf et al., 2015). Whether such highly dynamic hydrology and naturally extreme environment would compromise coral geochemical proxies was evaluated for the first time. Here, both monthly resolution and annual resolution records were obtained in recording runoff-associated changes, then water exchange and sediments transport and long-term variability of runoff were evaluated, helping to understand tidally controlled mixing and suspended sediment transport in such highly dynamical nearshore environment.

2. Oceanographic Setting

King Sound is a ~100-km-long embayment situated in the Kimberley, northwestern Australia (Figure 1), with one of the world's largest tidal regime with up to 12 m at spring tides. In the upper reaches of King Sound, Fitzroy River, the mightiest river in the Kimberley region, discharges into the bay near Derby (Figure 1a), delivering terrigenous sediments to the estuary forming an unusual tidal delta (Semeniuk & Brocx, 2011). It has, on average, the greatest volume of annual flow and the largest flood, with the mean of 5.75×10^9 m^3/year (Wolanski & Spagnol, 2003). Dominated by the Australian monsoon, rivers in the Kimberley region are subject to occasional, intense, and widespread rainfall, resulting in floods. The runoff of Fitzroy River is therefore highly related to seasonal changes in rainfall, with most of the discharge occurring in the wet season (i.e., Austral summer, from December to March) and the remainder of the year (dry season) negligible in terms of river and sediment runoff (Pusey & Kath, 2015). In addition, Fitzroy River is also characterized by high interannual variability in seasonal flows which can vary by orders of magnitude (Pusey & Kath, 2015).

Being a tide-dominated estuary, the exchange of riverine freshwater and sediment is restricted (Figure 1c). During the dry season, limited freshwater reaches offshore with a salinity maximum zone generated by evaporation in the upper reaches of the Sound, and as a result riverine sediments are mostly trapped in the upper regions (Figures 1b and 1c; Wolanski & Spagnol, 2003). During the wet season, observations in the adjacent Collier Bay have shown that freshwater input can extend some 50-km offshore under the influence of tidal pumping but with a prolonged residence time of around 60 days (Ivey et al., 2016). Comparison between the discharge of Fitzroy River, rainfall of the Cygnet Bay, and sea surface salinity (SSS; see details in section 3.4) of the nearshore region off the Sound indicates that coastal seawater is more readily affected by the influx of freshwater supplied by the Fitzroy River than precipitation, as the seasonal lowest salinity is correlated with the discharge peak ($r = -0.50$, $n = 17$; $p < 0.05$; Figure S2 in the supporting information) instead of rainfall peak ($r = -0.34$, $n = 20$; $p > 0.05$). Nevertheless, temporal lags exist between the time series, where river discharge led the salinity by ~2 months and lagged the rainfall in Cygnet Bay by ~1 month (Figure 2). Such a ~2-month lag is much longer than the typically delayed response time reported for estuary salinity, that is, 14–18 days for water exchange in the lower reaches within the estuary of axial length less than 100 km (Garvine et al., 1992; Lane et al., 2007) but is comparable to the observed extended residence time of freshwater in Collier Bay (Ivey et al., 2016). The time lag between rainfall and discharge is likely the result of variation of rainfall amount and timing across the catchment, as the Cygnet Bay is in the coastal region, while the Willare station locates landward.

3. Materials and Methods

3.1. Coral Sample Collection and Preparation

Coral cores KIM16 (massive *Porites* spp.) in this study were acquired in April 2016 from the subtidal zone of Shenton Bluff, Cygnet Bay, Kimberley region, Western Australia (Figure 1a). The cores were sliced into

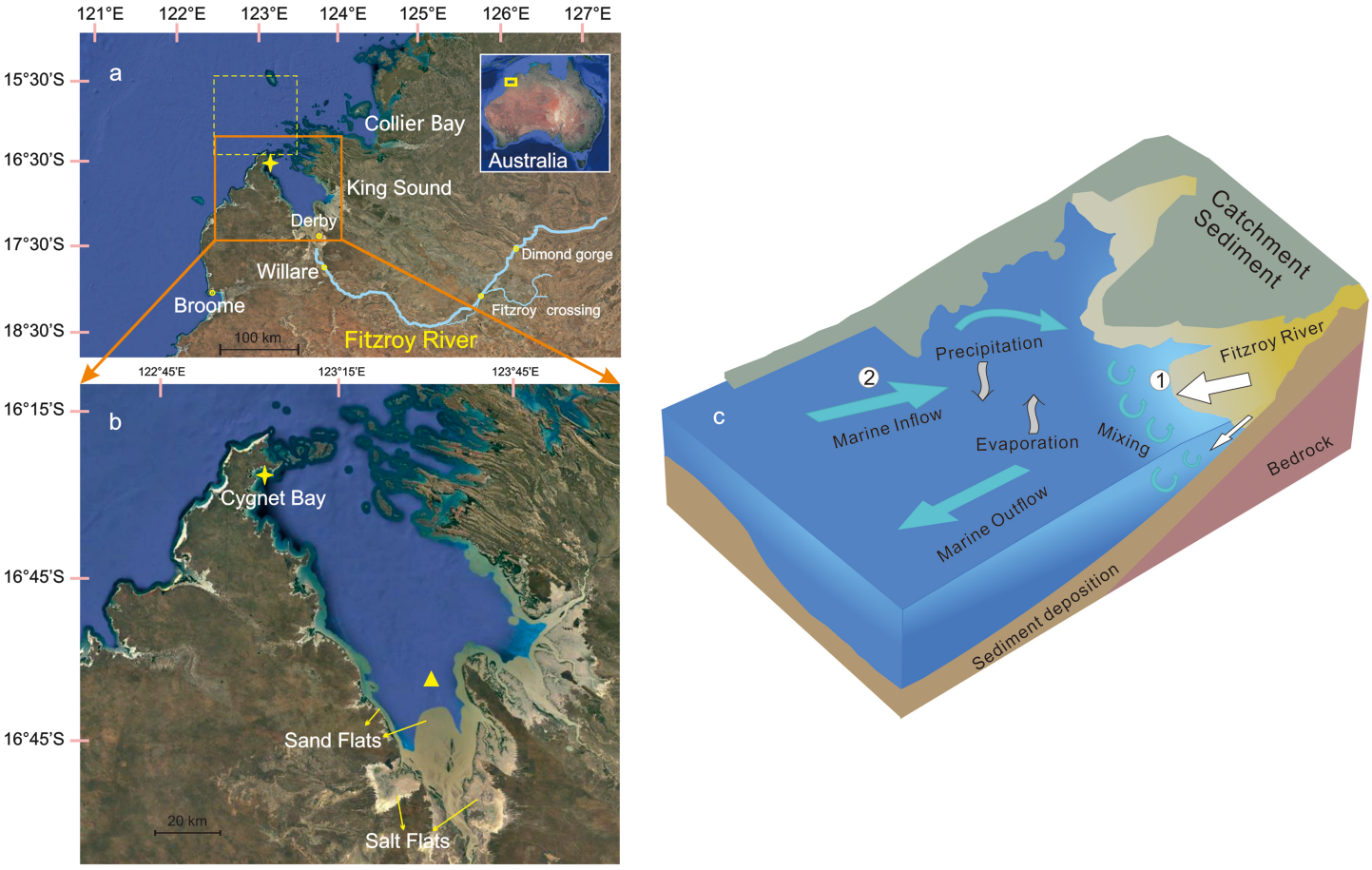

Figure 1. Study area. (a) Blue curve indicates the main stream of Fitzroy River, and the yellow star stands for the coral core sampling site. Dotted line marks the grid box for sea surface salinity data (see details in the text). (b) Inset of the orange box in (a). Yellow triangle stands for the salinity (turbidity) maximum zone observed by Wolanski and Spagnol (2003). (c) Schematic diagram for the hydrodynamics in the King Sound, modified from Ryan et al., (2003). Arrows indicate the transportation of seawater (blue arrows) and freshwater (white arrows). Major hydrodynamics marked with numbers: 1, freshwater input from the catchment with low volume relative to the total volume of water in the embayment, and the freshwater and terrestrial sediments (fine sediments) are most trapped near river mouth; 2, exchange of water between the embayment and the ocean dominates hydrological processes as a result of large tidal prism.

~7-mm-thick slabs along the plane of the vertical growth axis and X-rayed to reveal the density and annual growth bandings used as a guide for sampling (Figure S1). Detailed information of this coral refers to Chen et al., (2019). Before sampling, coral slabs were immersed in 6% reagent grade NaOCl for 24 hr to remove organic materials, followed with thoroughly rinse in an ultrasonic bath filled with deionized water and then dried at 40 °C.

Along the coral main growth axis, seasonal and annual samples were collected using a computer-controlled micromill, respectively. The top ~20 years (i.e., 1995–2015) of coral growth was milled at higher resolution with samples being collected at continuous intervals of ~1.4 mm (i.e., approximately eight subsamples per year). Before collecting annual samples, annual linear extension rates (1919 to 2015) were first measured across each of the light/dark annual bands in the X-ray images (Figure S1) and then used as a reference for the continuous sampling of annual increments down along the same milling path as seasonal subsamples.

3.2. Geochemical Analysis

Coral Ba/Ca ratios were measured at the University of Western Australia by using Q-ICPMS (X-series II, Thermo Fisher Scientific) following the method described by Holcomb et al. (2015). About 10-mg powders were dissolved in 0.51-M HNO_3, with subaliquots diluted in 2% HNO_3 spiked with a calibration solution to a final concentration of 10-ppm Ca (Holcomb et al., 2015). All HNO_3 was prepared from subboiling

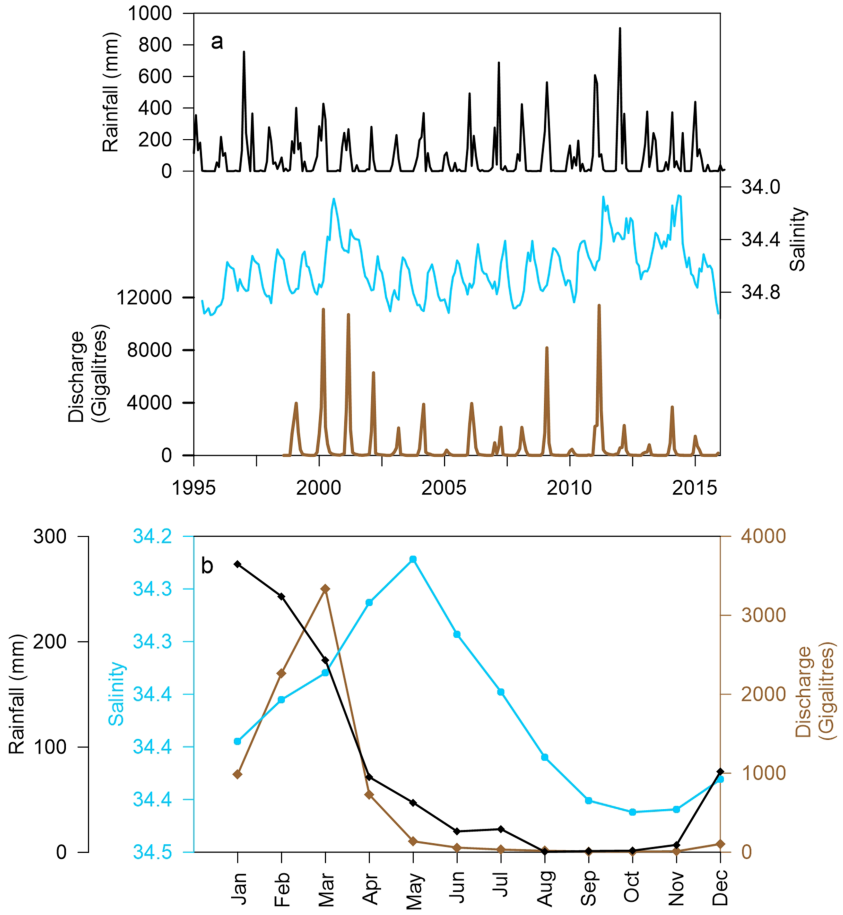

Figure 2. Comparison between Fitzroy River discharge, rainfall in the Cygnet Bay, and sea surface salinity (SSS) in the nearshore Kimberley: (a) monthly records from 1998 to 2016; (b) monthly mean records calculated from (a). Note that salinity is plotted on an inverted scale on the *y* axis to allow direct comparison with discharge and rainfall. Data sources are mentioned in the text.

distilled using a Savillex DST-1000. The coral standard JCp-1 was chemically treated and measured repeatedly along with the samples to monitor the analytical precision, which yielded a mean Ba/Ca value of 7.515 ± 0.205 (SD, $n = 15$) μmol/mol, consistent with the values reported in Hathorne et al. (2013).

Measurement for skeletal $\delta^{13}C$ and $\delta^{18}O$ was undertaken at the State Key Laboratory of Isotope Geochemistry, Guangzhou Institute of Geochemistry, following the methods described in Deng et al. (2009). The coral samples (~0.2 mg) were reacted with 102% H_3PO_4 at 90 °C to extract CO_2 in a MultiPrep® carbonate device and then measured on a GV Isoprime II stable isotope ratio mass spectrometer. Isotope data were normalized to the Vienna Pee Dee Belemnite using standard NBS-19 ($\delta^{13}C = 1.95‰$ and $\delta^{18}O = -2.20‰$). Repeated measurements ($n = 30$) of this standard yielded a standard deviation of 0.05‰ for $\delta^{13}C$ and 0.08‰ for $\delta^{18}O$.

3.3. Coral Geochemical Data Processing

3.3.1. Coral Residual $\delta^{18}O$ ($\Delta\delta^{18}O$)

To extract $\delta^{18}O_{sw}$-related information, residual $\delta^{18}O$ (i.e., $\Delta\delta^{18}O$) was calculated by subtracting the SST contribution from coral $\delta^{18}O$ values (Gagan et al., 1998) using the equation: $\Delta\delta^{18}O = d\delta^{18}O/dT \times [T_{\delta 18O} - T_{Sr/Ca}]$, where $d\delta^{18}O/dT$ is the slope of the empirical $\delta^{18}O$-SST function (0.23‰/°C, as reported by Gagan et al., (2012)), and $T_{\delta 18O}$ and $T_{Sr/Ca}$ are the apparent SSTs calculated from coral $\delta^{18}O$ and Sr/Ca values, respectively. The monthly resolved Sr/Ca-SST relationship of this coral (Chen et al., 2019) was used for $T_{Sr/Ca}$ calculation.

3.3.2. Coral Age Modal Construction

Coral growth chronology was constructed using Sr/Ca ratios, assuming that each Sr/Ca cycle represents 1 year and then correlating the Sr/Ca maximum and minimum within a year to the minimum and maximum monthly SST of the satellite records, respectively (Chen et al., 2019). As the coldest month (i.e., August) of a year is relatively constant, the maxima Sr/Ca were assigned as the "anchor points" to refine the age modals. Given that the high-resolution subsamples were milled at an interval of approximately eight samples per year, these seasonal series were linearly interpolated (via PAST software, Hammer et al., 2001) to convert the annual cycles with ≤12 data points to monthly resolution. The derived monthly time series were then used for correlation analysis with instrumental records and averaged to obtain the monthly mean of each record.

3.4. Climate and Environmental Data

The monthly SSS records were extracted from the U.K. Meteorological Office EN4 (UKMO EN4) data set on a 1° × 1° grid (grid box 122.5–123.5°E, 15.5–16.5°S) (Good et al., 2013). Data for Fitzroy River discharge were obtained from the Willare station, the nearest station to the Fitzroy River mouth (data available at the website: https://kumina.water.wa.gov.au/waterinformation/telem/stage.cfm). Data sets for solar exposure, wind speed, and precipitation were acquired from the Cygnet Bay bureau station (Bureau of Meteorology, Australia Government, http://www.bom.gov.au/climate/data/). Monthly sea level of Broome measured by tide gauge was also obtained from Bureau of Meteorology, Australia Government (http://www.bom.gov.au/oceanography/projects/ntc/monthly/index.shtml). Chlorophyll-*a* concentration data were generated by the National Oceanic Atmospheric Administration online database of Environmental Research Division Data Access Program, with the measurement gathered by the Moderate Resolution Imaging Spectroradiometer carried aboard the Aqua Spacecraft of National Aeronautics and Space Administration. The reconstructed Australian Monsoon Directional Index (AMDI) was obtained from Gallego et al. (2017), defined as [Dec (year^{-1}) + Jan (year) + Feb (year)] /3 standardized with respect to the 1800–2014 period.

4. Results

4.1. Monthly Coral Geochemical Records

Monthly coral $\delta^{18}O$, $\Delta\delta^{18}O$, $\delta^{13}C$, and Ba/Ca all exhibited pronounced seasonal variability but can be divided into two different categories: in-phase variation with Sr/Ca ($\delta^{18}O$) and out-of-phase variation with Sr/Ca ($\Delta\delta^{18}O$, $\delta^{13}C$, and Ba/Ca) (Figure 3). Therefore, strong correlation was only observed between $\delta^{18}O$ and Sr/Ca ($r = 0.75$, $n = 240$, $p < 0.01$), while Ba/Ca showed a weak positive relationship with Sr/Ca ($r = 0.36$, $n = 240$, $p < 0.01$), and no correlation was found for either $\Delta\delta^{18}O$ or $\delta^{13}C$ with Sr/Ca (Table 1).

As shown in Figure 3, major Ba/Ca peaks matched well with the $\Delta\delta^{18}O$ in terms of both timing and amplitude but to a less extent with $\delta^{13}C$. According to the chronological framework defined by Sr/Ca ratios, Ba/Ca peaks, as well as the lowest $\Delta\delta^{18}O$ and $\delta^{13}C$ values, mainly occurred in austral autumn months (i.e., from March to May), while $\delta^{18}O$ followed the variability of Sr/Ca with the lowest values occurring in austral summer months (i.e., from December to February) (Figure 3). The intercorrelation among $\Delta\delta^{18}O$, $\delta^{13}C$, and Ba/Ca are all significant ($p < 0.05$; Table 1). Negative correlation was noted between $\Delta\delta^{18}O$ and Ba/Ca with r of –0.67 ($n = 240$, $p < 0.01$) and between $\delta^{13}C$ and Ba/Ca with r of –0.40 ($n = 240$, $p < 0.01$). Despite the monthly mean records displayed synchronous variations in $\delta^{13}C$ and $\Delta\delta^{18}O$ (Figure 3), the correlation between them was weak ($r = 0.29$, $n = 240$, $p < 0.01$).

4.2. Annual Coral Geochemical Records

Remarkable secular decreasing trends were noted for $\delta^{13}C$ and $\delta^{18}O$ (or $\Delta\delta^{18}O$), with values shifting to the more depleted (Figure 4). Superimposed on these long-term trends, pronounced interannual to interdecadal variations were registered (Figure 4). As for Ba/Ca, the variation pattern was different. There was a tendency to large Ba/Ca peaks and enhanced baseline ratios from the 1920s (Figure 4). If we divide the time series into two different time blocks: before 1950 and after 1950, the baseline ratios increased from the range of 4.5–4.7 μmol/mol to a present-day range of 4.8–5.0 μmol/mol. The intercorrelations among these records were generally weak as illustrated in Table 1. Compared with the seasonal intercorrelations, reduced relationships were found between Ba/Ca and $\Delta\delta^{18}O$ ($r = -0.40$, $n = 99$, $p < 0.05$) and between $\delta^{18}O$ and

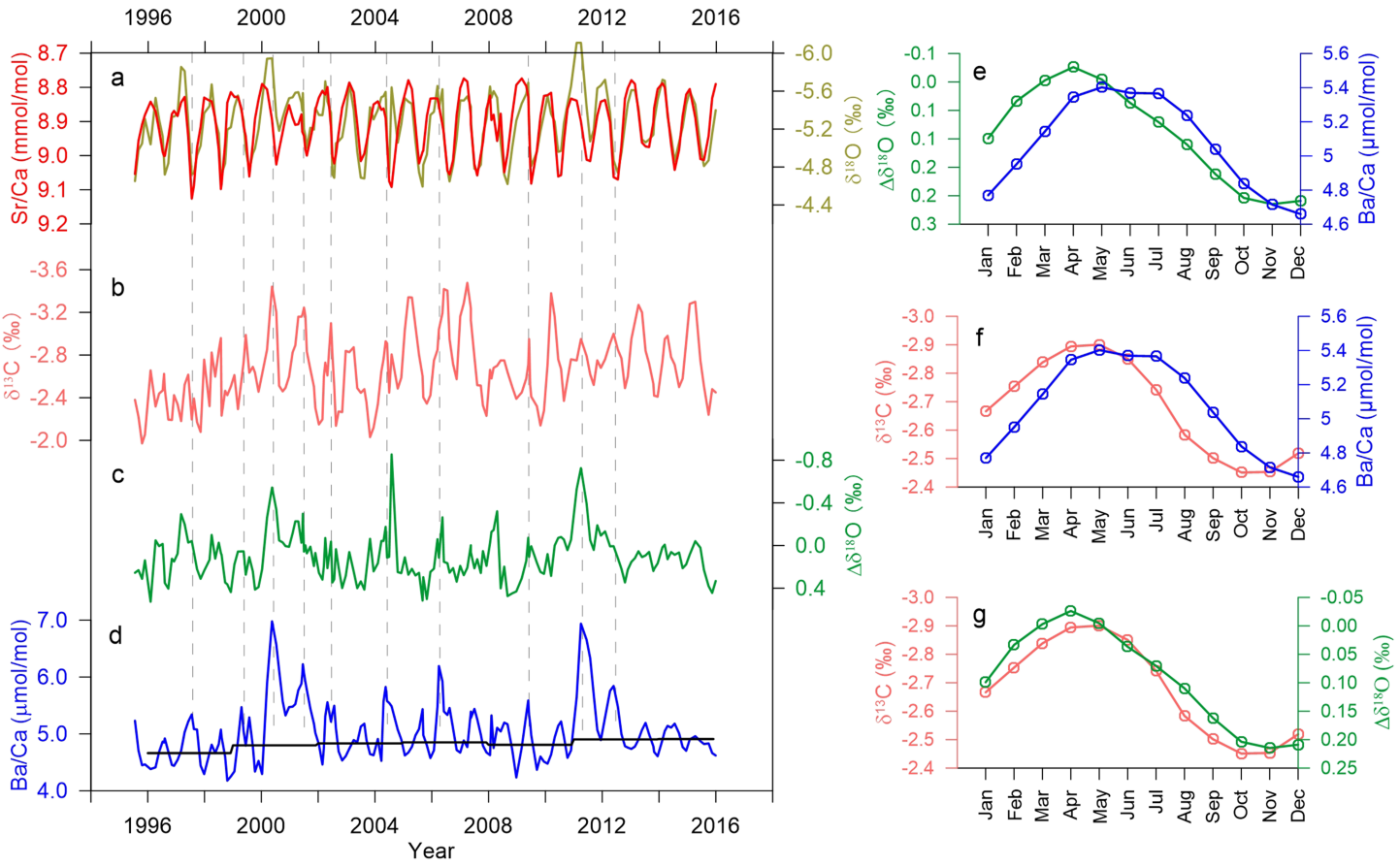

Figure 3. Monthly coral geochemical records from the nearshore Kimberley over the period of 1995 to 2015. Left panel: monthly time series of (a) $\delta^{18}O$ and Sr/Ca ratios; (b) $\delta^{13}C$; (c) $\Delta\delta^{18}O$; and (d) Ba/Ca. Right panel: monthly mean comparisons: (e) $\delta^{18}O$ versus Ba/Ca; (f) $\delta^{13}C$ versus Ba/Ca; and (g) $\delta^{13}C$ versus $\delta^{18}O$. The baseline changes for Ba/Ca ratios are denoted by the 3-year average of the monthly data with peak values >5.2 μmol/mol being first removed.

Sr/Ca ($r = 0.38$, $n = 99$, $p < 0.05$), while enhanced relationships were found between $\delta^{18}O$ and $\delta^{13}C$ ($r = 0.57$, $n = 99$, $p < 0.05$).

5. Discussion

5.1. Terrestrial Signal in Monthly Coral Geochemical Records

5.1.1. Ba/Ca Ratios

Coral Ba/Ca ratios exhibited regular seasonal peaks in austral autumn, fluctuating from ~4.1 to ~7.0 μmol/mol, with background values also exhibiting a marginal increase ($p < 0.01$) (Figure 3d). Such seasonal peaks and variation range are comparable to the previous reported Ba/Ca patterns in most corals across the Caribbean and Indo-Pacific regions, which are commonly attributed to the seasonal delivery of Ba by river runoff (Fallon et al., 1999; Jupiter et al., 2008; Lewis et al., 2018; McCulloch et al., 2003; Sinclair & McCulloch, 2004; Prouty et al., 2010; Saha, Rodriguez-Ramirez, et al., 2018), upwelling (Alibert & Kinsley, 2008; Lea et al., 1989; Reuer et al., 2003; Shen et al., 1992; Shen & Sanford, 1990), or groundwater (Alibert et al., 2003; Jiang et al., 2018).

In the estuary, river discharge and floods contribute greatly to the periodic spikes of Ba/Ca in coral skeletons (Fallon et al., 1999; McCulloch et al., 2003; Lewis et al., 2007, 2018; Sinclair & McCulloch, 2004). In our record, major Ba/Ca peaks also appeared to correspond to large discharge events

Table 1
Intercorrelations Among Coral Geochemical Records on Both Monthly and Annual Resolution

		$\delta^{18}O$	$\Delta\delta^{18}O$	$\delta^{13}C$	Sr/Ca
Seasonal	Ba/Ca	—	−0.67	−0.40	0.36
	$\delta^{18}O$		0.57	0.24	0.75
	$\Delta\delta^{18}O$			0.29	—
	$\delta^{13}C$				—
Annual	Ba/Ca	−0.27	−0.40	-	—
	$\delta^{18}O$		0.77	0.57	0.38
	$\Delta\delta^{18}O$			0.38	−0.28
	$\delta^{13}C$				0.31

Note. Correlation coefficients with p value below 0.05 are shown.

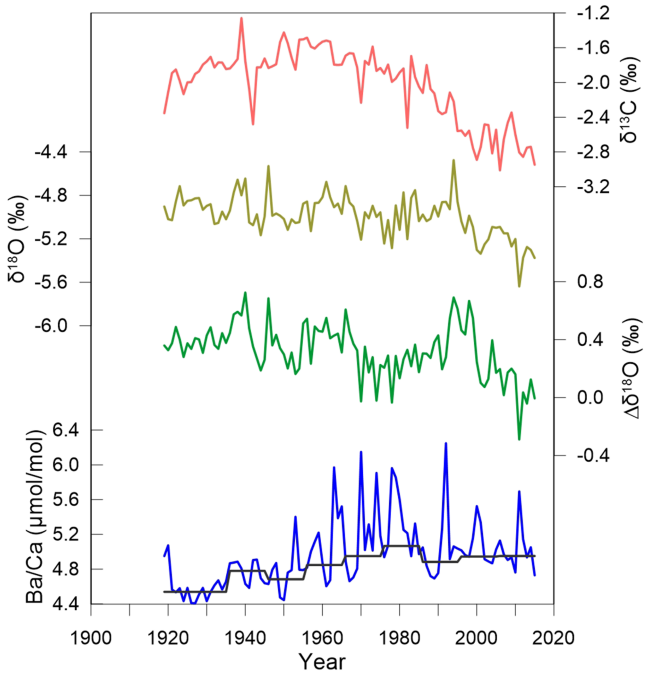

Figure 4. Annual coral geochemical records from the nearshore Kimberley over the period from 1919 to 2015. The baseline changes for Ba/Ca are denoted by the 10-year average of annual data with peak values >5.2 μmol/mol being first removed, exhibiting a significant increase from the 1920s with r of 0.82 ($p < 0.01$).

(Figure 5a), for example, during the enhanced runoff periods of 2000/2001, 2009, and 2011, despite a persistent temporal lag (1–2 months) that was noted between them. The monthly mean records showed that river discharge usually peaks at March, while coral Ba/Ca increases to its highest beginning at April and extending to July (Figure 5). This temporal lag likely leads to the reduced correlation relationship between coral Ba/Ca and discharge ($r = 0.24$, $n = 240$, $p < 0.05$; Table 2). Nevertheless, a strong correlation relationship ($r = 0.84$, $n = 17$, $p < 0.01$; Table 3) was noted between discharge peaks and the 1–2 months later Ba/Ca maximum (Figure S2), adding evidence to the hypothesis that coral Ba/Ca in King Sound is largely affected by the terrestrial runoff. This is also consistent with the seasonal variability of coastal salinity which changed in a similar manner with delayed response to heavy runoff occurring nearly 2 months later (Figure 2). Thus, coral Ba/Ca and salinity were found to display nearly concurrent variation (Figure 5), and the observed coral Ba/Ca peaks are interpreted as reflecting the seasonal input of riverine Ba (both dissolved and sediments desorbed Ba) from Fitzroy River to the nearshore region.

Such delayed responses of skeletal Ba/Ca to discharge have also been reported by Moyer et al., (2012), where they found coral Ba/Ca spikes lagged behind the peak discharge by about 1 to 2 months. Those authors have put forward several mechanisms to explain this temporal lag: (1) sporadic release of Ba from estuarine or floodplain-stored sediments, (2) dilution of the limited Ba supply by increased precipitation and river volume, and (3) slow growth rates leading to observed lags of trace metals in coral skeleton (Moyer et al., 2012 and the reference therein). In our study, this temporal lag has been observed in both SSS and coral Ba/Ca (also in $\Delta\delta^{18}O$ and $\delta^{13}C$; see following discussion), entailing a common factor or mechanism to explain such delayed response in both seawater and coral chemistry to river input. Therefore, the latter two possible mechanisms proposed by Moyer et al. (2012) can be ruled out in our case, as salinity changes also lag behind discharge (Figure 2) and coral growth in Kimberley is only slightly slower compared to those living in more typical and favorable tropical environment (Chen et al., 2019). Given that King Sound is a large macrotidal estuary and riverine sediments are mostly trapped in the upper reaches (Figure 1, Wolanski & Spagnol, 2003), it is likely that the sporadic release of Ba from the trapped sediments by tidal flushing would result in the slow transport of sediment and Ba in the Sound and lead to the observed lagged Ba/Ca peaks in coral skeleton. This also explains why Ba/Ca peaks also occurred when discharge input was small (e.g., 2005, 2010, and 2013), as the sediments trapped in the upper reaches serve as a permanent Ba source where tidal flushing facilitates the Ba release from it.

Nevertheless, we cannot rule out other possible factors that may produce such seasonal Ba/Ca signals like sediment resuspension, seepage of submarine groundwater, upwelling, or biological activity (e.g., coral spawning and phytoplankton blooms) (Alibert et al., 2003; Esslemont et al., 2004; Lea et al., 1989; Saha, Webb, et al., 2018). Given the sparse report and the unfavorable ocean conditions for upwelling along the western Australia coast (Varela et al., 2015), bottom seawater Ba transport is unlikely to be an important factor in the nearshore Kimberley. Additionally, wind-associated sediment resuspension seems to have small effects on coral Ba/Ca in this case, since a weak and inverse relationship ($r = -0.26$, $n = 177$, $p < 0.05$) was found between wind speed and coral Ba/Ca (Figure 5). Although it is not easy to fully evaluate the impacts of biological activity, satellite Chlorophyll-*a* concentration data were employed to compare with coral Ba/Ca time series (Figure 5). A weak but significant positive relationship was noted between Chlorophyll-*a* and Ba/Ca despite the variation patterns of them are divergent (Figure 5). This hints that phytoplankton blooms may have some effects on Ba/Ca peaks, as barite ($BaSO_4$) formation is thought to associate with such events. Nonetheless, this effect seems to be less important considering that in most studies such signal was commonly registered as sharp episodic Ba/Ca peaks (Gillikin et al., 2006; Sinclair, 2005).

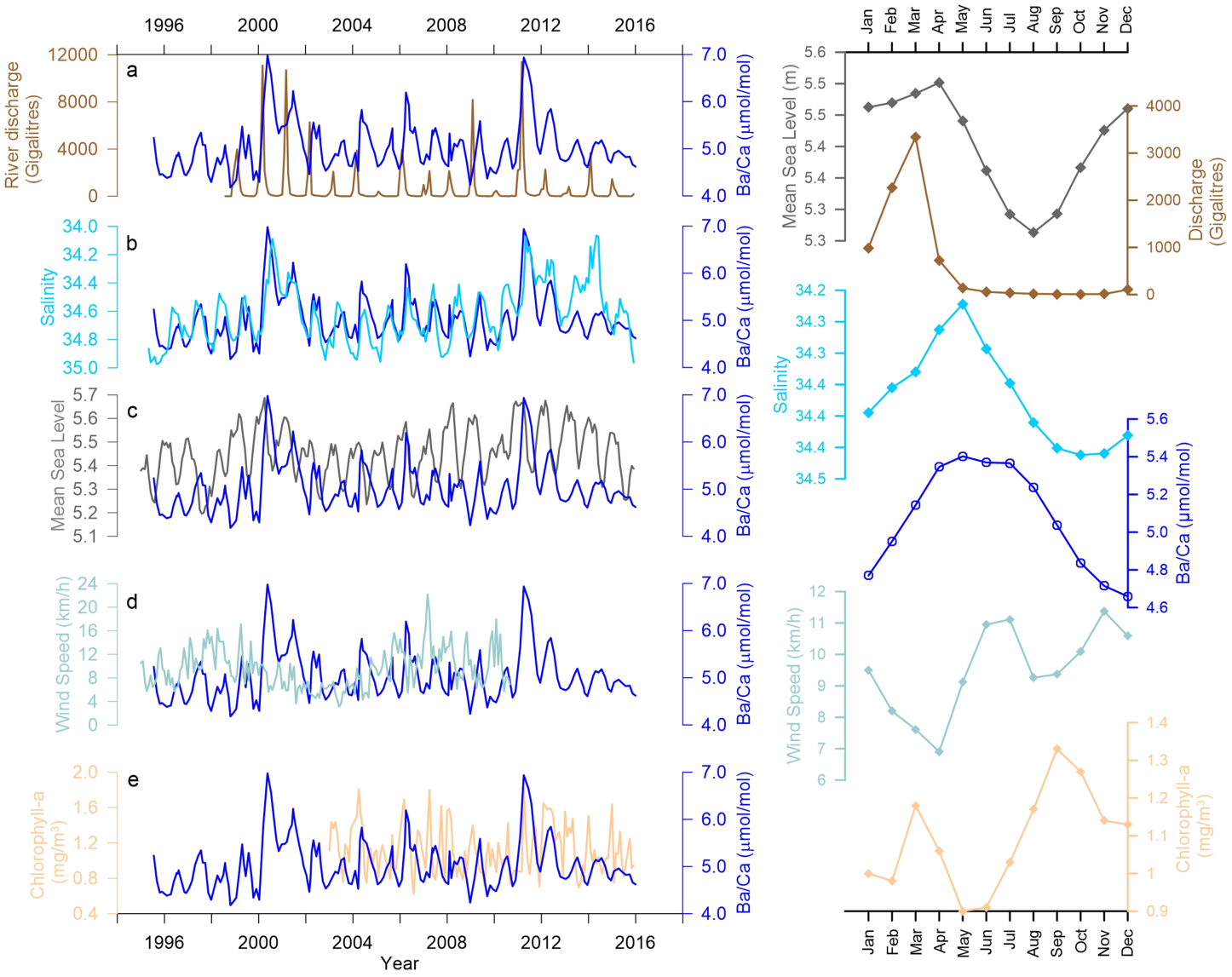

Figure 5. Left panel: monthly time series of (a) Ba/Ca ratios versus Fitzroy River discharge; (b) Ba/Ca ratios versus coastal salinity; (c) Ba/Ca ratios versus mean sea level gauged at Broome; (d) Ba/Ca ratios versus wind speed of Cygnet Bay, and (e) Ba/Ca ratios versus satellite Chlorophyll-*a* concentration. Right panel: Monthly mean records of all the variables in left panel. Note that salinity is plotted on an inverted scale on the *y* axis.

Table 2
Correlations Between Coral Geochemical Records and Environmental Variables

		Solar exposure	SSS	Discharge
Seasonal	Ba/Ca	—	−0.59	—
	$\delta^{18}O$	—	—	−0.46
	$\delta^{18}O$	—	0.39	−0.32
	$\delta^{13}C$	0.34	0.27	—
Annual	Ba/Ca	—	—	0.85
	$\delta^{18}O$	—	0.67	−0.52
	$\delta^{18}O$	—	0.52	—
	$\delta^{13}C$	—	0.41	—
	$\delta^{13}C$ detrended	—	0.39	—

Note. Correlation coefficients with *p* value below 0.05 are shown.

Lastly, another alternative factor is submarine groundwater, but it is difficult to assess its influences due to the shortage of groundwater data.

5.1.2. Coral Δ $\delta^{18}O$

The in-phase variations in coral $\delta^{18}O$ and Sr/Ca indicate that temperature accounts for a large part of seasonal variability of skeletal $\delta^{18}O$ for Kimberley coral, with about 56% variance being explained by Sr/Ca-derived SST (Table 1), leaving the remainder largely being affected by seawater $\delta^{18}O$ (henceforth $\delta^{18}O_{sw}$). After removing the temperature contribution, the derived $\Delta\delta^{18}O$ is then thought to be a proxy for seawater $\delta^{18}O_{sw}$. The nearly in-phase variation of coral $\Delta\delta^{18}O$ and coastal salinity as shown in Figure 6 corroborates that

Table 3
Correlations Between the Variation Amplitude of Coral Seasonal Geochemical Records and Environmental Variables

	Discharge	SSS	Precipitation
Ba/Ca	0.84	−0.45	—
$\Delta\delta^{18}O$	−0.73	0.68	—
$\delta^{13}C$	−0.45	0.48	—

Note. Correlation coefficients with p value below 0.05 are shown.

coral $\Delta\delta^{18}O$ rightly recorded the changes of $\delta^{18}O_{sw}$ in the lower reaches of King Sound, given that $\delta^{18}O_{sw}$ is commonly found to closely follow the variation of salinity (Conroy et al., 2017). However, a closer examination of the monthly time series found out that coral $\Delta\delta^{18}O$ led the coastal SSS by about 1 month (Figure 6) which is possibly induced by the slow water exchange due to that SSS data were obtained from the area ~20 km off the coral site.

Variability of $\delta^{18}O_{sw}$ is often inferred to be a result of regional precipitation, evaporation, runoff, advection, and upwelling (Conroy et al., 2017). In the King Sound, river runoff plays important role in defining the seasonality of salinity in the nearshore region. As a consequence, freshwater input of Fitzroy River likely also modulates the seasonal changes of $\delta^{18}O_{sw}$. Comparisons between $\Delta\delta^{18}O$ and Fitzroy River discharge and between $\Delta\delta^{18}O$ and Ba/Ca serve as evidence to support this argument, as monthly $\Delta\delta^{18}O$ covaried with Ba/Ca and appeared to follow the variability of discharge despite of the existence of persistent temporal lags (Figure 6). However, the correlations between $\Delta\delta^{18}O$ and SSS and between $\Delta\delta^{18}O$ and discharge are generally weak, with the coefficients of 0.40 ($n = 240$, $p < 0.05$; Table 2) and −0.32 ($n = 209$, $p < 0.05$; Table 2), respectively, likely induced by the small phase offsets found in the time series (Figure 6). Nevertheless, when plotting the discharge peak with the 1–2 months later $\Delta\delta^{18}O$ minimum, a strong negative relationship ($r = -0.73$, $n = 17$, $p < 0.01$; Table 3) was found which further demonstrates that the amplitude of seasonal $\Delta\delta^{18}O$ reduction was linked to that of

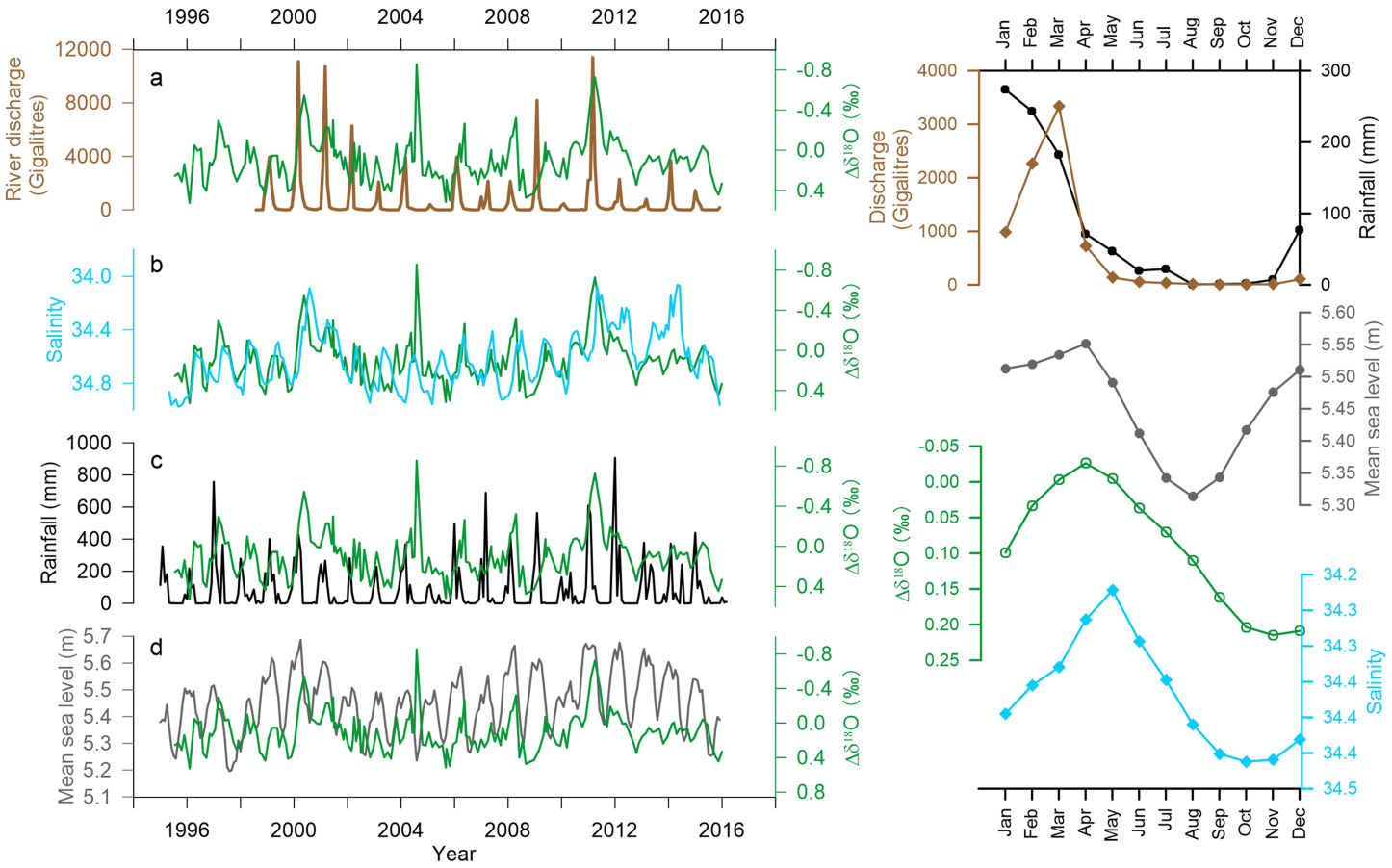

Figure 6. Left panel: monthly time series of (a) $\Delta\delta^{18}O$ versus Fitzroy River discharge; (b) $\Delta\delta^{18}O$ versus coastal salinity; (c) $\Delta\delta^{18}O$ versus rainfall of Cygnet Bay; and (d) $\Delta\delta^{18}O$ versus mean sea level gauged at Broome. Right panel: Monthly mean records of all the variables in left panel. Note that $\Delta\delta^{18}O$ and salinity are plotted on an inverted scale on the y axis.

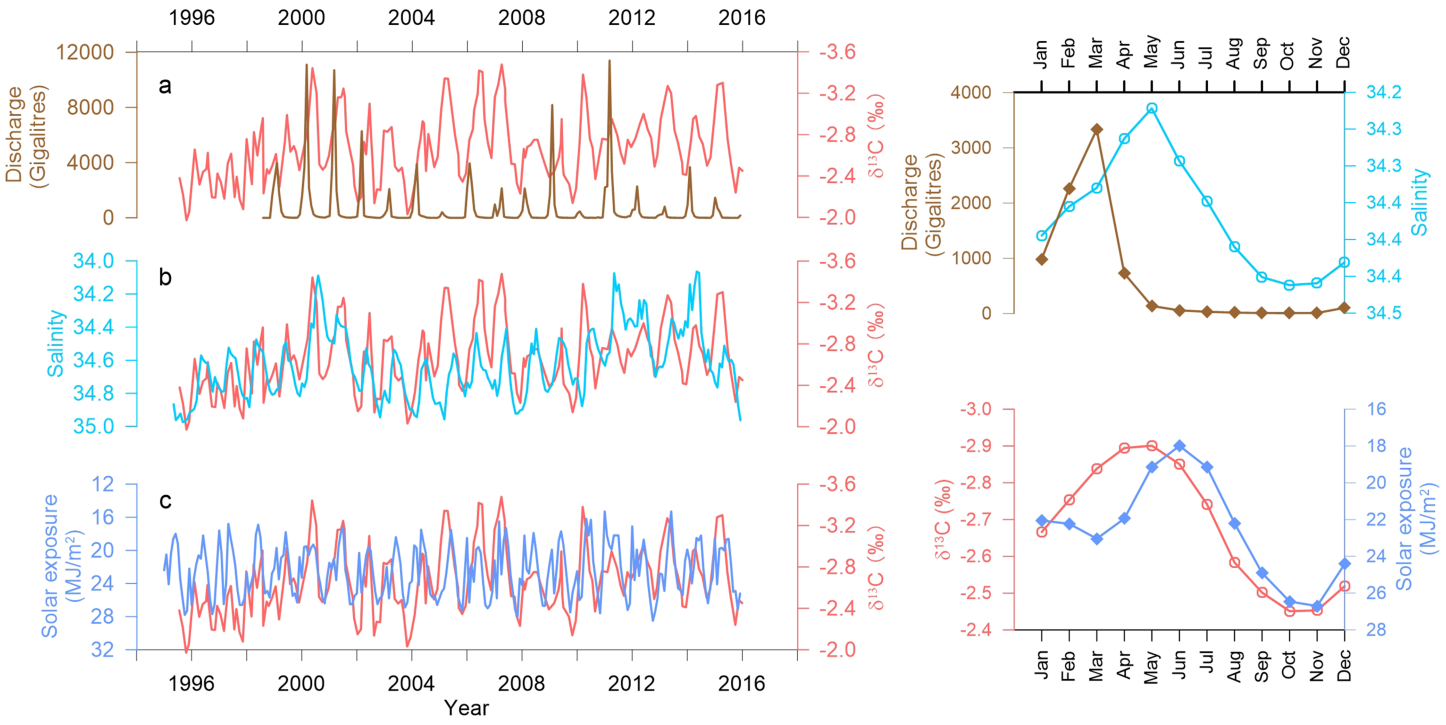

Figure 7. Left panel: Monthly time series comparisons: (a) $\delta^{13}C$ versus Fitzroy River discharge; (b) $\delta^{13}C$ versus coastal salinity; and (c) $\delta^{13}C$ versus solar exposure. Right panel: Monthly mean records of all the variables in left panel. Note that all the variables (except for discharge) are plotted on an inverted scale on the *y* axis.

discharge input and thus monthly coral $\Delta\delta^{18}O$ in the King Sound has been recording the freshwater influx supplied by Fitzroy River.

In addition to river runoff, precipitation would also reduce the $\delta^{18}O_{sw}$ value, but such effect seems to be less important in this case in particular on seasonal scales, since heavy rainfall periods did not always produce comparable $\Delta\delta^{18}O$ reductions (Figure 6c). Likewise, limited modulation was found for advection in that sea level variability was out-of-phase with both $\Delta\delta^{18}O$ and salinity as exhibited in Figure 6.

5.1.3. Coral $\delta^{13}C$

Unlike $\delta^{18}O$ and Ba/Ca, monthly variability of skeletal $\delta^{13}C$ in King Sound appeared to be complicated. Although it also varied seasonally and changed in phase with Ba/Ca and $\Delta\delta^{18}O$ (Figure 3), its variation pattern showed less clear runoff-associated signal compared to that of Ba/Ca and $\Delta\delta^{18}O$ (Figure 3). Lower $\delta^{13}C$ values tended to occur mainly in late austral summer to early autumn, showing evident phase offset with temperature cycles (Figure 2). This is manifested more clearly in the monthly mean records, where $\delta^{13}C$ lags behind temperature (or discharge) by about 1 month and changes simultaneously with $\Delta\delta^{18}O$ (Figure 7). As a result, no clear relationship was found between Sr/Ca and $\delta^{13}C$ or between $\delta^{18}O$ and $\delta^{13}C$, but weak correlations existed between $\delta^{13}C$ and Ba/Ca ratios and between $\delta^{13}C$ and $\Delta\delta^{18}O$ (Table 1). Since coral seasonal Ba/Ca and $\Delta\delta^{18}O$ in this study are mainly affected by Fitzroy River runoff, it is likely that the week relationships between them and $\delta^{13}C$ are also indicative of the runoff influences on coral $\delta^{13}C$. Further, a weak but significant negative relationship ($r = -0.45$, $n = 17$, $p < 0.05$; Table 3) was noted between discharge peaks and the 1–2 months later $\delta^{13}C$ minimum (Figure S2). As ^{13}C-depleted riverine DIC carried by runoff can reduce the carbon isotopic composition of seawater DIC, coral $\delta^{13}C$ would become more depleted in the wet seasons, along with the reductions in $\Delta\delta^{18}O$ and salinity and the elevation in Ba/Ca. Nevertheless, the weak relationship between $\delta^{13}C$ and Ba/Ca (or between $\delta^{13}C$ and $\Delta\delta^{18}O$) suggests that riverine influence can only explain a small part of $\delta^{13}C$ seasonal variability, and large discharge events did not always produce paralleled changes in $\delta^{13}C$ (Figure 7), implying that other factors may also control coral $\delta^{13}C$ variation in the nearshore Kimberley.

In addition to seawater DIC, metabolic CO_2 derived from photosynthesis and respiration accounts for another important DIC source in coral calcifying fluid where calcification takes place (Furla et al., 2000).

Therefore, any process affecting coral metabolism can also modulate the internal DIC and its carbon isotopic composition. Temperature and light are the most common factors driving coral metabolism, which could promote the rate of photosynthesis and respiration within certain ranges. As discussed above, $\delta^{13}C$ showed evident temporal lags with SST and display no clear correlation with Sr/Ca, indicating that temperature is unlikely to be the key factor driving coral internal $\delta^{13}C$ variation. We thus compared the $\delta^{13}C$ with local solar exposure and found that $\delta^{13}C$ covaried with the seasonal cycles of solar exposure, with higher $\delta^{13}C$ values occurring during higher solar exposure periods and lower $\delta^{13}C$ values occurring during lower solar exposure periods (Figure 7). Such light-driven $\delta^{13}C$ variations have been reported in many previous studies (Grottoli, 2002; Swart, Leder, et al., 1996; Weil et al., 1981), a result of the light-enhanced photosynthesis which consumes more ^{12}C-enriched CO_2 and leaves the internal C pool enriched in ^{13}C. However, with respect to the monthly mean records of $\delta^{13}C$ and solar exposure, it seems that $\delta^{13}C$ is more readily affected by river runoff in the wet season as elevated solar irradiation does not produce parallel changes in coral $\delta^{13}C$ (Figure 7). Therefore, for Kimberley coral, we proposed that both river input and photosynthesis drive the seasonal variations in skeletal $\delta^{13}C$.

5.1.4. Implications for Water and Sediments Transport in King Sound

Delayed responses (~1–2 months) of coastal SSS and coral geochemistry to Fitzroy River runoff demonstrate that water mixing and sediments transport in King Sound are generally restricted and slow compared to the common reported mixing time for river-dominated estuaries (Garvine et al., 1992; Lane et al., 2007). This is consistent with the previous observation that freshwater and fine sediment were mostly restricted in the upper reaches of the Sound (Wolanski & Spagnol, 2003). Given that King Sound is a tide-dominated estuary, tide-induced circulation is thought to have large effects on the flow of freshwater and suspended sediment seaward from the estuary (Allen et al., 1980; Ryan et al., 2003). For example, large tidal exchange can buffer the effects of floods. During wet seasons, exceptionally high meteorological tides ("King tides") that produced by the onshore winds and spring tides can pile oceanic water into the Sound (Jennings, 1975) and thereby likely prevent the transport of the freshwater coming down the Fitzroy River. As can be seen from the Figure 5 (or Figure 6), discharge peaks rightly corresponded to the highest sea level periods, partially demonstrating that inflow of large amount of freshwater and seawater occurred simultaneously in the Sound. Thus, this possibly leads to the observed lagged responses of seawater $\delta^{18}O_{sw}$ and SSS to river runoff. Meanwhile, tidal movement affects sedimentation and seaward escape of suspended sediment, which creates a tidal sediment trap in the upper estuary, and results in extended residence time of fine sediment (Ivey et al., 2016; Wolanski & Spagnol, 2003). The field observation in adjacent Collier Bay provides supportive evidence that the retention time for water and sediments in such macrotidal environment is much longer, varying from 20 to 140 days depending on the topography, with average time of around 60 days (Ivey et al., 2016). This is induced by the dominant macrotidal forcing and the complex topography/bathymetry of the estuary which together produce the complex residual circulation driving the flushing and particles transport in the estuary (Ivey et al., 2016). Therefore, it is possible that such macrotidal forcing and the topography/bathymetry of King Sound could also produce a similar water and sediment transport situation leading to the observed temporal lags in water chemistry in the lower reaches of the estuary. Further, riverine sediment (even the fine sediment) largely trapped in the upper regions of King Sound by tidal pumping (Wolanski & Spagnol, 2003) is consistent with the observation in Collier Bay that most sediments delivered by river and/or freshwater are also stored in the upper reach of estuary, preventing the instant exchange with seawater in the lower reaches (Ivey et al., 2016).

5.2. Annual Variations in Coral $\delta^{18}O$, $\delta^{13}C$, and Ba/Ca Records

Given only 18-year data available for the Fitzroy River discharge at Willare station, it is unsafe to fully evaluate the responses of coral skeletal geochemistry to terrestrial inputs on annual scales. Nevertheless, it appeared that large discharge peaks in 2000 and 2011 have produced corresponding signals on coral Ba/Ca ratios (Figure 8). As a result, annual Ba/Ca ratios showed a strong and significant relationship with discharge ($r = 0.85$, $n = 18$, $p < 0.01$), highlighting the control of river input on estuary Ba concentrations in King Sound. As such, notably reductions in $\delta^{18}O$ and coastal salinity also occurred during these two heavy discharge periods, likely resulting in the weak but significant negative correlations between discharge and coral $\delta^{18}O$ ($r = -0.52$, $n = 18$, $p < 0.01$) and between discharge and salinity ($r = -0.48$, $n = 18$, $p < 0.01$).

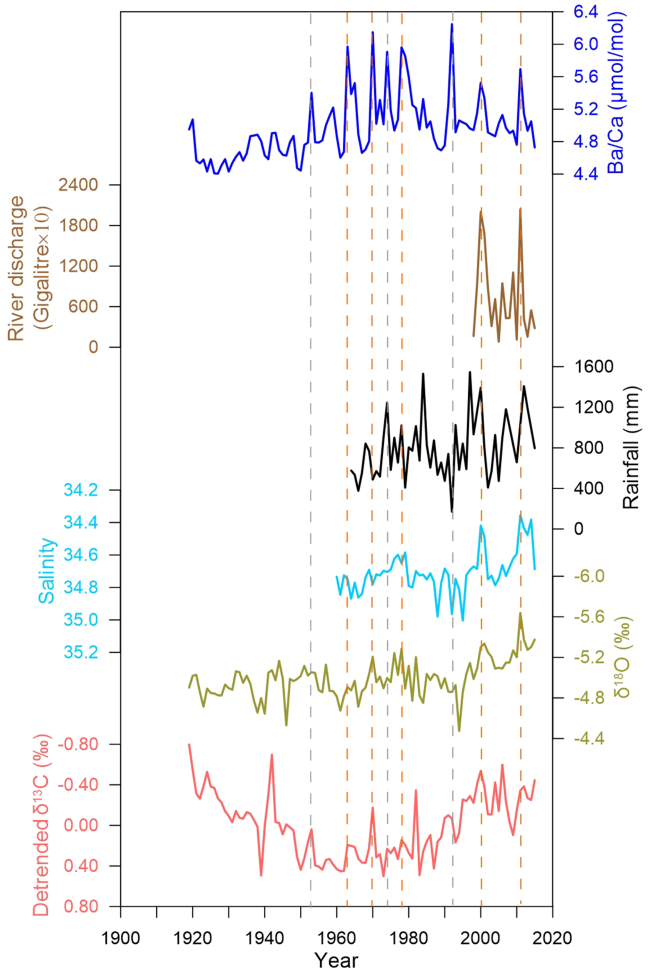

Figure 8. Annual variations in coral geochemical and instrumental records. The orange dashed lines denote the synchronized changes in all the time series if available, while the gray denotes the out-of-step changes. Note that $\delta^{18}O$, salinity, and $\delta^{13}C$ are plotted on an inverted scale on the *y* axis to allow for visual comparison.

On the annual scales, $\delta^{18}O$ was closely related to the variability of salinity with correlation coefficient of 0.67 ($n = 52$, $p < 0.01$) and less affected by temperature ($r = 0.38$, $n = 97$, $p < 0.01$), hinting that SSS accounted for the majority (~45%) variance of annual $\delta^{18}O$ (Table 2). Therefore, these concurrent reductions in $\delta^{18}O$ and salinity suggest the influence of freshwater on nearshore seawater chemistry. In addition, rainfall also displayed similar variation pattern with heavy rainfall occurring during these two periods (Figure 8), and negative relationships were noted between it and $\delta^{18}O$ ($r = -0.32$, $n = 47$, $p < 0.05$) and between it and salinity ($r = -0.47$, $n = 47$, $p < 0.01$). This suggests that freshwater influx signal registered by coral annual $\delta^{18}O$ record in King Sound was linked to rainfall-associated runoff. Despite that the 2000 and 2011 runoff signals are captured by both coral Ba/Ca and $\delta^{18}O$ (as well as salinity), larger Ba/Ca peaks before 1990s (i.e., 1992, 1978, 1974, 1970, and 1963) did not always correspond to comparable shifts in coral $\delta^{18}O$ or salinity records. This is possibly due to the less control of discharge on $\delta^{18}O$ or salinity, but with only 18-year discharge data it is not confident to evaluate the underlying mechanism of the occasional decoupling of them. Nonetheless, this may indicate that the runoff-related information hold by annual records are less straightforward compared to seasonal data.

With respect to $\delta^{13}C$, terrestrial signal is less manifested on annual time series. The long-term decreasing trend is often attributed to the addition of ^{13}C-depleted anthropogenic CO_2 into the ocean, namely, the Suess effect (Deng et al., 2017; Swart et al., 2010; Linsley et al., 2019). To better understand local environmental effects on coral $\delta^{13}C$, this background trend was removed by the PAST software. The detrended $\delta^{13}C$ time series exhibited no significant correlation with either Ba/Ca or river discharge, but weak relationships are found between it and $\delta^{18}O$ ($r = 0.33$, $n = 97$, $p< 0.01$) and between it and SSS ($r = 0.39$, $n = 56$, $p < 0.01$). This may be indicative of less important contribution of river DIC input for the estuary seawater on annual timescales.

5.3. Possible Linkage to Australia Summer Monsoon

Long-term decreasing trend of $\delta^{18}O$ ($\Delta\delta^{18}O$) and increased Ba/Ca baseline ratios as well as variation amplitude all point to enhanced runoff influx to the Sound, which is likely linked to the strengthened monsoon precipitation in the northern Australia (a result of intensification of the total cloud amount and the extension of monsoon rainforest; Bowman et al., 2010; Jovanovic et al., 2011; Smith, 2004; Taschetto & England, 2009). To evaluate the long-term influence of Monsoon precipitation, we adopted AMDI (Gallego et al., 2017) to compare with the coral records. This index is found to have linkage with rainfall changes over all tropical Australia and parts of the semiarid terrains in Western Australia (Gallego et al., 2017). Although no significant correlation was found between AMDI and coral geochemical data (or rainfall in Cygnet Bay), after applied a 5-year running average to all time series significant correlations were found between AMDI and coral records (as well as rainfall) (Table 4 and Figure 9). This possibly highlights the linkage of rainfall and runoff in King Sound to the Australian Monsoon over interannual to interdecadal timeframe, suggesting that strengthened monsoon precipitation has likely increased the terrestrial input and freshwater to the nearshore Kimberley region.

Table 4
Correlations Among Coral Geochemical Records, Precipitation, and AMDI

	Precipitation		AMDI	
	Annual	5-year average	Annual	5-year average
Ba/Ca	—	—	—	0.32
$\delta^{18}O$	−0.31	−0.63	—	−0.41
$\Delta\delta^{18}O$	—	−0.37	—	−0.33
Precipitation			—	0.48

Note. Correlation coefficients with *p* value below 0.05 are shown.

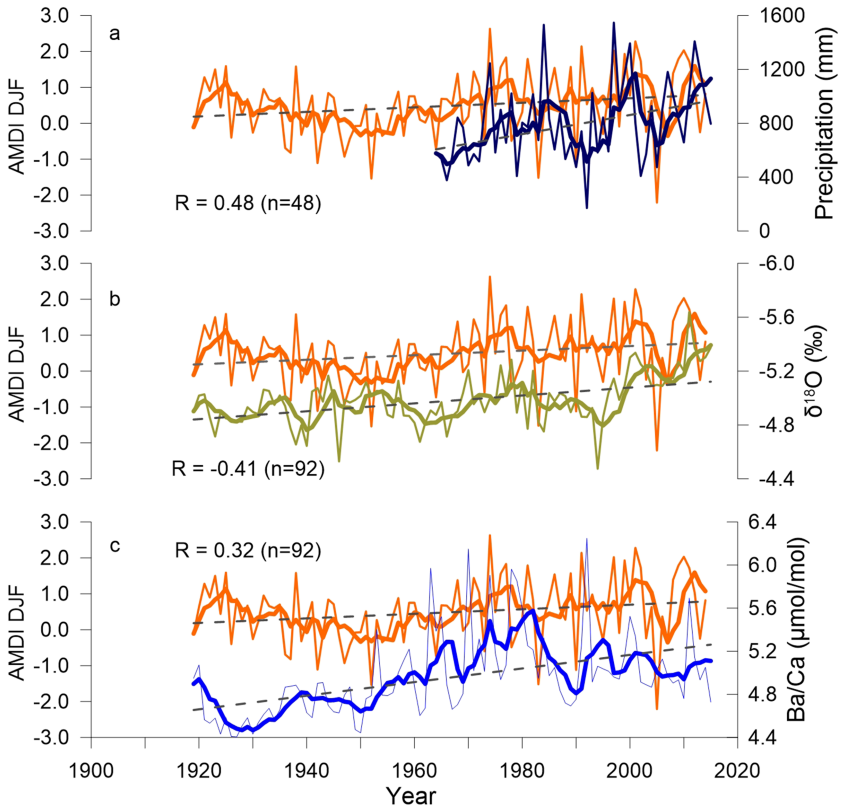

Figure 9. Comparisons among Australian monsoon and local records for Cygnet Bay: (a) precipitation; (b) $\delta^{18}O$; (c) Ba/Ca ratios. Bold lines indicate the 5-year average of each record with significant ($p < 0.05$) long-term trends shown in dashed lines. The correlation coefficients for 5-year averaged AMDI and coral geochemical records are shown with $p > 0.05$.

Acknowledgments
The authors would like to thank Dr. Juan Pablo D'Olivo and Dr. Xi Liu for their assistance on geochemical analysis. Thanks also go to the Editor Miguel Goni and two anonymous reviewers for their incisive and constructive comments. This work was supported by funding provided by an ARC Laureate Fellowship (LF120100049) awarded to Professor Malcolm McCulloch, the ARC Centre of Excellence for Coral Reef Studies (CE140100020), the National Key Research and Development Program of China (2016YFA0601204), and the National Natural Science Foundation of China (41803017 and 41722301), and Key Special Project for Introduced Talents Team of Southern Marine Science and Engineering Guangdong Laboratory (Guangzhou) (GML2019ZD0308). This is contribution IS-2804 from GIG-CAS. Data sets for this article can be found at Chen et al. (2019): Monthly and annual coral Barium/Calcium, δ18O, and δ13C records from a macrotide dominated nearshore reef environment, Kimberley region of northwestern Australia. PANGAEA (https://doi.org/10.1594/PANGAEA.907586).

6. Conclusions

High-resolution and annually resolved coral Ba/Ca, $\delta^{18}O$, and $\delta^{13}C$ series from the nearshore Kimberley region were utilized to explore their applicability in recording river runoff in highly dynamic and thermally extreme environment. Terrestrial signatures are well manifested in monthly Ba/Ca and $\Delta\delta^{18}O$ records but to a lesser extent in monthly $\delta^{13}C$ records. The temporal lag found between river discharge and skeletal geochemical records (as well as coastal salinity) suggests a prolonged water and sediments transport in King Sound, possibly due to the extraordinary macrotidal forcing in the Kimberley region. For the annual records, Ba/Ca and $\delta^{18}O$ are still affected by the river runoff, while the ^{13}C Suess effects dominate the variation of $\delta^{13}C$. Additionally, $\delta^{18}O$ exhibited a long-term downward trend, while Ba/Ca showed progressively upward trend from 1920s onward, coupled with the increased Australian monsoon and precipitation, suggesting that enhanced monsoon precipitation has brought more freshwater and sediment loads to the nearshore Kimberley region.

References

Alibert, C., & Kinsley, L. (2008). A 170-year Sr/Ca and Ba/Ca coral record from the western Pacific warm pool: 2. A window into variability of the New Ireland Coastal Undercurrent? *Journal of Geophysical Research*, *113*, C04008. https://doi.org/10.1029/2006JC003979

Alibert, C., Kinsley, L., Fallon, S. J., McCulloch, M. T., Berkelmans, R., & McAllister, F. (2003). Source of trace element variability in Great Barrier Reef corals affected by the Burdekin flood plumes. *Geochimica et Cosmochimica Acta*, *67*(2), 231–246.

Allen, G. P., Salomon, J. C., Bassoullet, P., Penhoat, Y. D., & de Grandpré, C. (1980). Effects of tides on mixing and suspended sediment transport in macrotidal estuaries. *Sedimentary Geology*, *26*(1-3), 59–90. https://doi.org/10.1016/0037-0738(80)90006-8

Allison, N., & Finch, A. A. (2012). A high resolution δ13C record in a modern Porites lobata coral: Insights into controls on skeletal $\delta^{13}C$. *Geochimica et Cosmochimica Acta*, *84*(0), 534–542. https://doi.org/10.1016/j.gca.2012.02.004

Bowman, D. M. J. S., Murphy, B. P., & Banfai, D. S. (2010). Has global environmental change caused monsoon rainforests to expand in the Australian monsoon tropics? *Landscape Ecology*, *25*(8), 1247–1260. https://doi.org/10.1007/s10980-010-9496-8

Carroll, J., Falkner, K. K., Brown, E. T., & Moore, W. S. (1993). The role of the Ganges-Brahmaputra mixing zone in supplying barium and ^{226}Ra to the Bay of Bengal. *Geochimica et Cosmochimica Acta*, *57*(13), 2981–2990. https://doi.org/10.1016/0016-7037(93)90287-7

Chen, T., Yu, K., Li, S., Chen, T., & Shi, Q. (2011). Anomalous Ba/Ca signals associated with low temperature stresses in Porites corals from Daya Bay, northern South China Sea. *Journal of Environmental Sciences*, *23*(9), 1452–1459. https://doi.org/10.1016/S1001-0742(10)60606-7

Chen, X., D'Olivo, J. P., Wei, G., & McCulloch, M. (2019). Anthropogenic ocean warming and acidification recorded by Sr/Ca, Li/Mg, δ11B and B/Ca in Porites coral from the Kimberley region of northwestern Australia. *Palaeogeography, Palaeoclimatology, Palaeoecology*, *528*, 50–59. https://doi.org/10.1016/j.palaeo.2019.04.033

Chow, T. J., & Goldberg, E. D. (1960). On the marine geochemistry of barium. *Geochimica et Cosmochimica Acta*, *20*(3–4), 192–198. https://doi.org/10.1016/0016-7037(60)90073-9

Coffey, M., Dehairs, F., Collette, O., Luther, G., Church, T., & Jickells, T. (1997). The behaviour of dissolved barium in estuaries. *Estuarine, Coastal and Shelf Science*, *45*(1), 113–121. https://doi.org/10.1006/ecss.1996.0157

Cole, J. E., Fairbanks, R. G., & Shen, G. T. (1993). Recent variability in the southern oscillation: Isotopic results from a Tarawa atoll coral. *Science*, *260*(5115), 1790–1793. https://doi.org/10.1126/science.260.5115.1790

Conroy, J. L., Thompson, D. M., Cobb, K. M., Noone, D., Rea, S., & Legrande, A. N. (2017). Spatiotemporal variability in the δ^{18}O-salinity relationship of seawater across the tropical Pacific Ocean. *Paleoceanography*, *32*(5), 484–497. https://doi.org/10.1002/2016PA003073

Dandan, S. S., Falter, J. L., Lowe, R. J., & McCulloch, M. T. (2015). Resilience of coral calcification to extreme temperature variations in the Kimberley region, northwest Australia. *Coral Reefs*, *34*(4), 1151–1163. https://doi.org/10.1007/s00338-015-1335-6

Deng, W., Chen, X., Wei, G., Zeng, T., & Zhao, J.-X. (2017). Decoupling of coral skeletal δ^{13}C and solar irradiance over the past millennium caused by the oceanic Suess effect. *Paleoceanography*, *32*(2), 161–171. https://doi.org/10.1002/2016PA003049

Deng, W., Wei, G., Xie, L., & Yu, K. (2013). Environmental controls on coral skeletal δ^{13}C in the northern South China Sea. *Journal of Geophysical Research: Biogeosciences*, *118*(4), 1359–1368. https://doi.org/10.1002/jgrg.20116

Deng, W.-F., Wei, G.-J., Li, X.-H., Yu, K.-F., Zhao, J.-X., Sun, W.-D., & Liu, Y. (2009). Paleoprecipitation record from coral Sr/Ca and δ^{18}O during the mid-Holocene in the northern South China Sea. *The Holocene*, *19*(6), 811–821. https://doi.org/10.1177/0959683609337355

Edmond, J. M., Boyle, E. D., Drummond, D., Grant, B., & Mislick, T. (1978). Desorption of barium in the plume of the Zaire (Congo) river. *Netherlands Journal of Sea Research*, *12*(3), 324–328. https://doi.org/10.1016/0077-7579(78)90034-0

Esslemont, G., Russell, R. A., & Maher, W. A. (2004). Coral record of harbour dredging: Townsville, Australia. *Journal of Marine Systems*, *52*(1), 51–64. https://doi.org/10.1016/j.jmarsys.2004.01.005

Fairbanks, R. G. (1982). The origin of continental shelf and slope water in the New York Bight and Gulf of Maine: evidence from $H_2{}^{18}O/H_2{}^{16}O$ ratio measurements. *Journal of Geophysical Research*, *87*, 5796–5808.

Fallon, S. J., McCulloch, M. T., van Woesik, R., & Sinclair, D. J. (1999). Corals at their latitudinal limits: Laser ablation trace element systematics in Porites from Shirigai Bay, Japan. *Earth and Planetary Science Letters*, *172*(3), 221–238. https://doi.org/10.1016/S0012-821X(99)00200-9

Felis, T., Suzuki, A., Kuhnert, H., Dima, M., Lohmann, G., & Kawahata, H. (2009). Subtropical coral reveals abrupt early-twentieth-century freshening in the western North Pacific Ocean. *Geology*, *37*(6), 527–530. https://doi.org/10.1130/G25581A.1

Furla, P., Galgani, I., Durand, I., & Allemand, D. (2000). Sources and mechanisms of inorganic carbon transport for coral calcification and photosynthesis. *J ExpBiol*, *203*(22), 3445–3457.

Gagan, M. K., Ayliffe, L. K., Hopley, D., Cali, J. A., Mortimer, G. E., Chappell, J., et al. (1998). Temperature and surface-ocean water balance of the mid-Holocene tropical western Pacific. *Science*, *279*(5353), 1014–1018. https://doi.org/10.1126/science.279.5353.1014

Gallego, D., García-Herrera, R., Peña-Ortiz, C., & Ribera, P. (2017). The steady enhancement of Australian Summer Monsoon in the last 200 years. *Scientific Reports*, *7*(1), 1–7. https://doi.org/10.1038/s41598-017-16414-1

Garvine, R. W., McCarthy, R. K., & Wong, K.-C. (1992). The axial salinity distribution in the delaware estuary and its weak response to river discharge, Estuarine. *Coastal and Shelf Science*, *35*(2), 157–165. https://doi.org/10.1016/S0272-7714(05)80110-6

Gillikin, D. P., Dehairs, F., Lorrain, A., Steenmans, D., Baeyens, W., & André, L. (2006). Barium uptake into the shells of the common mussel (Mytilus edulis) and the potential for estuarine paleo-chemistry reconstruction. *Geochimica et Cosmochimica Acta*, *70*(2), 395–407. https://doi.org/10.1016/j.gca.2005.09.015

Gonneea, M. E., Cohen, A. L., DeCarlo, T. M., & Charette, M. A. (2017). Relationship between water and aragonite barium concentrations in aquaria reared juvenile corals. *Geochimica et Cosmochimica Acta*, *209*, 123–134. https://doi.org/10.1016/j.gca.2017.04.006

Good, S. A., Martin, M. J., & Rayner, N. A. (2013). EN4: Quality controlled ocean temperature and salinity profiles and monthly objective analyses with uncertainty estimates. *Journal of Geophysical Research: Oceans*, *118*(12), 6704–6716. https://doi.org/10.1002/2013JC009067

Grottoli, A. G. (2002). Effect of light and brine shrimp on skeletal δ^{13}C in the Hawaiian coral Porites compressa: A tank experiment. *Geochimica et Cosmochimica Acta*, *66*(11), 1955–1967. https://doi.org/10.1016/S0016-7037(01)00901-2

Grove, C. A., Zinke, J., Scheufen, T., Maina, J., Epping, E., Boer, W., et al. (2012). Spatial linkages between coral proxies of terrestrial runoff across a large embayment in Madagascar. *Biogeosciences*, *9*, 3063–3081. https://doi.org/10.5194/bg-9-3063-2012

Guo, Y., Deng, W., Chen, X., Wei, G., Yu, K., & Zhao, J.-x. (2016). Saltier sea surface water conditions recorded by multiple mid-Holocene corals in the northern South China Sea. *Journal of Geophysical Research: Oceans*, *121*(8), 6323–6330. https://doi.org/10.1002/2016JC012034

Hammer, Ø., Harper, D. A. T., & Ryan, P. D. (2001). PAST: Paleontological statistics software package for education and data analysis. *Palaeontologia Electronica*, *4*, 1–9.

Hathorne, E. C., Gagnon, A., Felis, T., Adkins, J., Asami, R., Boer, W., et al. (2013). Interlaboratory study for coral Sr/Ca and other element/Ca ratio measurements, Geochemistry, Geophysics. *Geosystems*, *14*(9), 3730–3750. https://doi.org/10.1002/ggge.20230

Hendy, E. J., Gagan, M. K., Alibert, C. A., McCulloch, M. T., Lough, J. M., & Isdale, P. J. (2002). Abrupt decrease in tropical Pacific sea surface salinity at end of Little Ice Age. *Science*, *295*(5559), 1511–1514. https://doi.org/10.1126/science.1067693

Holcomb, M., DeCarlo, T. M., Schoepf, V., Dissard, D., Tanaka, K., & McCulloch, M. (2015). Cleaning and pre-treatment procedures for biogenic and synthetic calcium carbonate powders for determination of elemental and boron isotopic compositions. *Chemical Geology*, *398*, 11–21. https://doi.org/10.1016/j.chemgeo.2015.01.019

Horta-Puga, G., & Carriquiry, J. D. (2012). Coral Ba/Ca molar ratios as a proxy of precipitation in the northern Yucatan Peninsula, Mexico. *Applied Geochemistry*, *27*(8), 1579–1586. https://doi.org/10.1016/j.apgeochem.2012.05.008

Ivey, G., Brinkman, R., Lowe, R., Jones, N., Symonds, G., & Espinosa-Gayosso, A. (2016). Physical oceanographic dynamics in the Kimberley. *Final Report for WAWSI Kimberley Marine Research Program, Project*, *2*(2), 1.

Jennings, J. N. (1975). Desert dunes and estuarine fill in the Fitzroy estuary (North-Western Australia). *Catena*, *2*, 215–262. https://doi.org/10.1016/S0341-8162(75)80015-4

Jiang, W., Yu, K., Song, Y., Zhao, J.-X., Feng, Y.-X., Wang, Y., & Xu, S. (2018). Coral geochemical record of submarine groundwater discharge back to 1870 in the northern South China Sea. *Palaeogeography, Palaeoclimatology, Palaeoecology*, *507*, 30–38. https://doi.org/10.1016/j.palaeo.2018.05.045

Jovanovic, B., Collions, D., Braganza, K., Jakob, D., & Jones, D. A. (2011). A high-quality monthly tital cloud amount dataset for Australia. *Climatic Change*, *108*(3), 485–517. https://doi.org/10.1007/s10584-010-9992-5

Jupiter, S., Roff, G., Marion, G., Henderson, M., Schrameyer, V., McCulloch, M., & Hoegh-Guldberg, O. (2008). Linkages between coral assemblages and coral proxies of terrestrial exposure along a cross-shelf gradient on the southern Great Barrier Reef. *Coral Reefs*, *27*(4), 887–903. https://doi.org/10.1007/s00338-008-0422-3

Lane, R. R., Day, J. W., Marx, B. D., Reyes, E., Hyfield, E., & Day, J. N. (2007). The effects of riverine discharge on temperature, salinity, suspended sediment and chlorophyll *a* in a Mississippi delta estuary measured using a flow-through system, Estuarine. *Coastal and Shelf Science*, *74*(1), 145–154. https://doi.org/10.1016/j.ecss.2007.04.008

LaVigne, M., Grottoli, A. G., Palardy, J. E., & Sherrell, R. M. (2016). Multi-colony calibrations of coral Ba/Ca with a contemporaneous in situ seawater barium record. *Geochimica et CosmochimicaActa*, *179*, 203–216. https://doi.org/10.1016/j.gca.2015.12.038

Lea, D. W., Shen, G. T., & Boyle, E. A. (1989). Coralline barium records temporal variability in equatorial Pacific upwelling. *Nature*, *340*(6232), 373–376.

Lewis, S. E., Brodie, J. E., McCulloch, M. T., Mallela, J., Jupiter, S. D., Stuart Williams, H., et al. (2012). An assessment of an environmental gradient using coral geochemical records, Whitsunday Islands, Great Barrier Reef, Australia. *Marine Pollution Bulletin*, *65*(4), 306–319. https://doi.org/10.1016/j.marpolbul.2011.09.030

Lewis, S. E., Lough, J. M., Cantin, N. E., Matson, E. G., Kinsley, L., Bainbridge, Z. T., & Brodie, J. E. (2018). A critical evaluation of coral Ba/Ca, Mn/Ca and Y/Ca ratios as indicators of terrestrial input: New data from the Great Barrier Reef, Australia. *Geochimica et Cosmochimica Acta*, *237*, 131–154. https://doi.org/10.1016/j.gca.2018.06.017

Lewis, S. E., Shields, G. A., Kamber, B. S., & Lough, J. M. (2007). A multi-trace element coral record of land-use changes in the Burdekin River catchment, NE Australia, Palaeogeography, Palaeoclimatology. *Palaeoecology*, *246*(2), 471–487. https://doi.org/10.1016/j.papaeo.2006.10.021

Linsley, B. K., Dunbar, R. B., Dassié, E. P., Tangri, N., Wu, H. C., Brenner, L. D., & Wellington, G. M. (2019). Coral carbon isotope sensitivity to growth rate and water depth with paleo-sea level implications. *Nature Communications*, *10*(1), 2056. https://doi.org/10.1038/s41467-019-10054-x

Lough, J. M., Lewis, S. E., & Cantin, N. E. (2015). Freshwater impacts in the central Great Barrier Reef: 1648-2011. *Coral Reefs*, *34*(3), 739–751. https://doi.org/10.1007/soo338-015-1297-8

Maina, J., de Moel, H., Vermaat, J. E., HenrichBruggemann, J., Guillaume, M. M. M., Grove, C. A., et al. (2012). Linking coral river runoff proxies with climate variability, hydrology and land-use in Madagascar catchments. *Marine Pollution Bulletin*, *64*(10), 2047–2059. https://doi.org/10.1016/j.marpolbul.2012.06.027

McConnaughey, T. A. (2003). Sub-equilibrium oxygen-18 and carbon-13 levels in biological carbonates: Carbonate and kinetic models. *Coral Reefs*, *22*(4), 316–327. https://doi.org/10.1007/s00338-003-0325-2

McConnaughey, T. A., Burdett, J., Whelan, J. F., & Paull, C. K. (1997). Carbon isotopes in biological carbonates: Respiration and photosynthesis. *Geochimica et Cosmochimica Acta*, *61*(3), 611–622. https://doi.org/10.1016/S0016-7037(96)00361-4

McCulloch, M., Fallon, S., Wyndham, T., Hendy, E., Lough, J., & Barnes, D. (2003). Coral record of increased sediment flux to the inner Great Barrier Reef since European settlement. *Nature*, *421*(6924), 727–730. https://doi.org/10.1038/nature01361

McCulloch, M. T., Gagan, M. K., Mortimer, G. E., Chivas, A. R., & Isdale, P. J. (1994). A high-resolution Sr/Ca and δ18O coral record from the Great Barrier Reef, Australia, and the 1982–1983 El Niño. *Geochimica et Cosmochimica Acta*, *58*(12), 2747–2754. https://doi.org/10.1016/0016-7037(94)90142-2

Moore, W. S., & Shaw, T. J. (2008). Fluxes and behavior of radium isotopes, barium, and uranium in seven Southeastern US rivers and estuaries. *Marine Chemistry*, *108*(3), 236–254. https://doi.org/10.1016/j.marchem.2007.03.004

Moyer, R. P., Grottoli, A. G., & Olesik, J. W. (2012). A multiproxy record of terrestrial inputs to the coastal ocean using minor and trace elements (Ba/Ca, Mn/Ca, Y/Ca) and carbon isotopes ($\delta^{13}C$, $\Delta^{14}C$) in a nearshore coral from Puerto Rico. *Paleoceanography*, *27*(3). https://doi.org/10.1029/2011PA002249

Nguyen, A. D., Zhao, J. X., Feng, Y. X., Hu, W., Yu, K., Gasparon, M., et al. (2013). Impact of recent coastal development and human activities on Nha Trang Bay, Vietnam: Evidence from a Porites lutea geochemical record. *Coral Reefs*, *32*(1), 181–193. https://doi.org/10.1007/s00338-012-0962-4

Prouty, N. G., Field, M. E., Stock, H. D., Jupiter, S. D., & McCulloch, M. (2010). Coral Ba/Ca records of sediment input to the fringing reef of the southshore of Molaka'i, Hawai'i over the last several decades. *Marine Pollution Bulletin*, *60*(10), 1822–1835. https://doi.org/10.1016/j.marpolbul.2010.05.024

Prouty, N. G., Hughen, K. A., & Carilli, J. (2008). Geochemical signature of land-based activities in Caribbean coral surface samples. *Coral Reefs*, *27*(4), 727–742. https://doi.org/10.1007/s00338-008-0413-4

Pusey, B. J., & Kath, J. (2015). *Environmental water management in the Fitzroy River Valley information availability, knowledge gaps and research needs*. National Environmental Science Programme: Northern Australia Environmental Resources Hub.

Reuer, M. K., Boyle, E. A., & Cole, J. E. (2003). A mid-twentieth century reduction in tropical upwelling inferred from coralline trace element proxies. *Earth and Planetary Science Letters*, *210*(3), 437–452. https://doi.org/10.1016/S0012-821X(03)00162-6

Richards, Z. T., Garcia, R. A., Wallace, C. C., Rosser, N. L., & Muir, P. R. (2015). A diverse assemblage of reef corals thriving in a dynamic intertidal reef setting (Bonaparte Archipelago, Kimberley, Australia). *PLoS ONE*, *10*(2), e0117791. https://doi.org/10.1371/journal.pone.0117791

Ryan, D. A., Heap, A. D., Radke, L., & Heggie, D. T. (2003). Conceptual models of Australia's estuaries and coastal waterways: Applications for coastal resource management. Geoscience Austraia, Record 2003/09, 136 pp.

Sackett, W. M., Netratanawong, T., & Holmes, E. M. (1997). Carbon-13 variations in the dissolved inorganic carbon in estuarine waters. *Geophysical Research Letters*, *24*(1), 21–24. https://doi.org/10.1029/96GL03694

Saha, N., Rodriguez-Ramirez, A., Nguyen, A. D., Clark, T. R., Zhao, J.-X., & Webb, G. E. (2018). Seasonal to decadal scale influence of environmental drivers on Ba/Ca and Y/Ca in coral aragonite from the southern Great Barrier Reef. *Sci Total Environ*, *639*, 1099–1109. https://doi.org/10.1016/j.scitotenv.2018.05.156

Saha, N., Webb, G. E., & Zhao, J.-X. (2016). Coral skeletal geochemistry as a monitor of inshore water quality. *Sci Total Environ*, *566-567*, 652–684. https://doi.org/10.1016/j.scitotenv.2016.05.066

Saha, N., Webb, G. E., Zhao, J.-X., Leonard, N. D., & Nguyen, A. D. (2018). Influence of marine biochemical cycles on seasonal variation of Ba/Ca in the near-shore coral Cyphastrea, Rat Island, southern Great Barrier Reef. *Chemical Geology*, *499*, 71–83. https://doi.org/10.1016/j.chemgeo.2018.09.005

Schoepf, V., Stat, M., Falter, J. L., & McCulloch, M. T. (2015). Limits to the thermal tolerance of corals adapted to a highly fluctuating, naturally extreme temperature environment. *Scientific Reports*, *5*, 17639. https://doi.org/10.1038/srep17639

Semeniuk, V., & Brocx, M. (2011). King sound and the tide-dominated delta of the Fitzroy river: Their geoheritage values. *Journal of the Royal Society of Western Australia*, *94*(2), 151–160.

Shen, G., & Sanford, C. (1990). Trace element indicators of climate variability in reef-building corals, Global Ecological Consequences of the 1982–83 El Nino–Southern Oscillation. *Elsevier Oceanography Series*, *52*, 255–283. https://doi.org/10.1016/S0422-9894(08)70038-2

Shen, G. T., Cole, J. E., Lea, D. W., Linn, L. J., McConnaughey, T. A., & Fairbanks, R. G. (1992). Surface ocean variability at Galapagos from 1936–1982: Calibration of geochemical tracers in corals. *Paleoceanography*, *7*(5), 563–588. https://doi.org/10.1029/92PA01825

Sinclair, D. J. (2005). Non-river flood barium signals in the skeletons of corals from coastal Queensland, Australia. *Earth and Planetary Science Letters*, *237*(3), 354–369. https://doi.org/10.1016/j.epsl.2005.06.039

Sinclair, D. J., & McCulloch, M. T. (2004). Corals record low mobile barium concentrations in the Burdekin River during the 1974 flood: Evidence for limited Ba supply to rivers? Palaeogeography, Palaeoclimatology. *Palaeoecology*, *214*(1–2), 155–174. https://doi.org/10.1016/j.palaeo.2004.07.028

Smith, I. (2004). An assessment of recent trends in Australian rainfall. *Australian Meteorological Magazine*, *53*, 163–173.

Swart, P. K., Greer, L., Rosenheim, B. E., Moses, C. S., Waite, A. J., Winter, A., et al. (2010). The ^{13}C Suess effect in scleractinian corals mirror changes in the anthropogenic CO_2 inventory of the surface oceans. *Geophysical Research Letters*, *37*(5). https://doi.org/10.1029/2009GL041397

Swart, P. K., Healy, G., Greer, L., Lutz, M., Saied, A., Anderegg, D., et al. (1999). The use of proxy chemical records in Coral skeletons to ascertain past environmental conditions in Florida Bay. *Estuaries*, *22*(2), 384–397. https://doi.org/10.2307/1353206

Swart, P. K., Healy, G. F., Dodge, R. E., Kramer, P., Hudson, J. H., Halley, R. B., & Robblee, M. B. (1996). The stable oxygen and carbon isotopic record from a coral growing in Florida Bay: A 160-year record of climatic and anthropogenic influence, Palaeogeography, Palaeoclimatology. *Palaeoecology*, *123*(1–4), 219–237. https://doi.org/10.1016/0031-0182(95)00078-X

Swart, P. K., Leder, J. J., Szmant, A. M., & Dodge, R. E. (1996). The origin of variations in the isotopic record of scleractinian corals: II. Carbon. *Geochimica et Cosmochimica Acta*, *60*(15), 2871–2885. https://doi.org/10.1016/0016-7037(96)00119-6

Tanzil, J. T. I., Goodkin, N. F., Sin, T. M., Chen, M. L., Fabbro, G. N., Boyle, E. A., et al. (2019). Multi-colony coral skeletal Ba/Ca from Singapore's turbid urban reefs: Relationship with contemporaneous in-situ seawater parameters. *Geochimica et Cosmochimica Acta*, *250*, 191–208. https://doi.org/10.1016/j.gca.2019.01.034

Taschetto, A. S., & England, M. H. (2009). An analysis of late twentieth century trends in Australian rainfall. *International Journal of Climatology*, *29*, 791–807. https://doi.org/10.1002/joc.1736

Tudhope, A. W., Lea, D. W., Shimmield, G. B., Chilcott, C. P., & Head, S. (1996). Monsoon climate and Arabian Sea coastal upwelling recorded in massive corals from southern Oman. *PALAIOS*, *347-361*. https://doi.org/10.2307/3515245

Varela, R., Álvarez, I., Santos, F., deCastro, M., & Gómez-Gesteira, M. (2015). Has upwelling strengthened along worldwide coasts over 1982-2010? *Sci Rep-Uk*, *5*, 10016. https://doi.org/10.1038/srep10016

Walther, B. D., & Nims, M. K. (2015). Spatiotemporal variation of trace elements and stable isotopes in subtropical estuaries: I. Freshwater endmembers and mixing curves. *Estuaries and Coasts*, *38*(3), 754–768. https://doi.org/10.1007/s12237-014-9881-7

Weil, S. M., Buddemeier, R. W., Smith, S. V., & Kroopnick, P. M. (1981). The stable isotopic composition of coral skeletons: Control by environmental variables. *Geochimica et Cosmochimica Acta*, *45*(7), 1147–1153. https://doi.org/10.1016/0016-7037(81)90138-1

Wolanski, E., & Spagnol, S. (2003). Dynamics of the turbidity maximum in King Sound, tropical Western Australia, Estuarine. *Coastal and Shelf Science*, *56*(5), 877–890. https://doi.org/10.1016/S0272-7714(02)00214-7

Wolgemuth, K., & Broecker, W. S. (1970). Barium in sea water. *Earth and Planetary Science Letters*, *8*(5), 372–378. https://doi.org/10.1016/0012-821X(70)90110-X

Wyndham, T., McCulloch, M., Fallon, S., & Alibert, C. (2004). High-resolution coral records of rare earth elements in coastal seawater: Biogeochemical cycling and a new environmental proxy. *Geochimica et Cosmochimica Acta*, *68*(9), 2067–2080. https://doi.org/10.1016/j.gca.2003.11.004